

way things are manufactured in the composite industry. It enables the production of large-scale composite tooling with good surface finish, tight tolerances and the ability to withstand autoclave processing in just a few days. For instance, a single piece monolithic hull of a yacht was fabricated using multi-axis robotic arms fitted with carbon filament extruder head.<sup>9</sup> The design flexibility of 3D printing allowed sophisticated weaving and careful control of the fiber tows into the shape of hull optimized for specialized loading and performance conditions. It demonstrates the prospect of 3D printed composite materials to be used in place of heavy metals to produce a part. Apart from that, 3D printing could further expand the use of composite materials toward multifunctional structures. Multicomponent structures with embedded functionality can be built in a single print. The ability to print CNT and silver conductive ink<sup>10</sup> and continuous copper wires opens up the possibility to realize embedded circuits or electronics for structural health monitoring and de-icing.

Although still in the early stage, composite 3D printing is gaining traction

within the manufacturing industry. It provides a quick and automated approach to manufacturing composite parts, which used to be labor-intensive and require highly skilled operators to make. Composite 3D printing pushes the re-evaluation of the material choice for some applications, replacing metals with equally strong and cheaper polymer composites. The tool-free fabrication technique for composite not only makes the process of fabricating composite parts much faster and less costly, but also opens up the possibility of multifunctional composite structures for new applications. These advantages will surely motivate the adoption and development of 3D printing technology as part of standard techniques in the future of composite maker's toolkit.

1. Yap, Y.L., and Yeong, W.Y. (2014). Additive manufacture of fashion and jewellery products: a mini review. *Virtual and Physical Prototyping* 9, 195–201.
2. Sriram, V., Shukla, V., and Biswas, S. (2019). "Metal Powder Based Additive Manufacturing Technologies—Business Forecast," in *3D Printing and Additive Manufacturing Technologies*, L.J. Kumar, P.M. Pandey, and D.I. Wimpenny, eds. (Springer Singapore), pp. 105–118.

3. Chapiro, M. (2016). Current achievements and future outlook for composites in 3D printing. *Reinforced Plastics* 60, 372–375.
4. Yap, Y.L., Wang, C., Sing, S.L., Dikshit, V., Yeong, W.Y., and Wei, J. (2017). Material jetting additive manufacturing: An experimental study using designed metrological benchmarks. *Precision Engineering* 50, 275–285.
5. Goh, G.D., Yap, Y.L., Agarwala, S., and Yeong, W.Y. (2019). Recent Progress in Additive Manufacturing of Fiber Reinforced Polymer Composite. *Adv. Mater. Technol.* 4.
6. Qiao, J., Li, Y., and Li, L. (2019). Ultrasound-assisted 3D printing of continuous fiber-reinforced thermoplastic (F RTP) composites. *Additive Manufacturing* 30, 100926.
7. Luo, M., Tian, X., Shang, J., Yun, J., Zhu, W., Li, D., and Qin, Y. (2020). Bi-scale interfacial bond behaviors of CCF/PEEK composites by plasma-laser cooperatively assisted 3D printing process. *Compos. Part A Appl. Sci. Manuf.* 131, 105812.
8. Shi, B., Shang, Y., Zhang, P., Cuadros, A.P., Qu, J., Sun, B., Gu, B., Chou, T.-W., and Fu, K. (2019). Dynamic Capillary-Driven Additive Manufacturing of Continuous Carbon Fiber Composite. *Matter* 2, this issue, 1594–1604.
9. Musio-Sale, M., Nazzaro, P.L., and Peterson, E. (2020). Visions, Concepts, and Applications in Additive Manufacturing for Yacht Design (Springer International Publishing), pp. 401–410.
10. Goh, G.L., Agarwala, S., and Yeong, W.Y. (2019). Directed and On-Demand Alignment of Carbon Nanotube: A Review toward 3D Printing of Electronics. *Adv. Mater. Interfaces* 6, 1801318.

## Introduce Tortuosity to Retain Polysulfides and Suppress Li Dendrites

Jiashen Meng,<sup>1,3</sup> Quan Pang,<sup>2,3,\*</sup> and Liqiang Mai<sup>1,\*</sup>

**Practical application of lithium-sulfur batteries remains challenging, including issues with both cathode and anode. Recently in *Matter*, researchers report a novel solution for sulfur cathode and lithium anode, introducing tortuosity into a graphene-oxide host, resulting in significant performance improvement.**

The use of lithium-sulfur (Li-S) battery as one of the most promising energy storage systems has attracted great interests

because of its high theoretical capacity, high abundance, and low cost.<sup>1</sup> As shown in [Figure 1A](#), a common configuration of

Li-S battery is composed of a Li anode, electrolyte, separator, and sulfur cathode. Three major scientific problems in Li-S batteries lead to their poor

<sup>1</sup>State Key Laboratory of Advanced Technology for Materials Synthesis and Processing, Wuhan University of Technology, Wuhan 430070, China

<sup>2</sup>College of Engineering, and Beijing Innovation Center for Engineering Science and Advanced Technology, Peking University, Beijing 100871, China

<sup>3</sup>These authors contributed equally

\*Correspondence:  
pangquan@coe.pku.edu.cn (Q.P.),  
mlq518@whut.edu.cn (L.M.)  
<https://doi.org/10.1016/j.matt.2020.05.007>



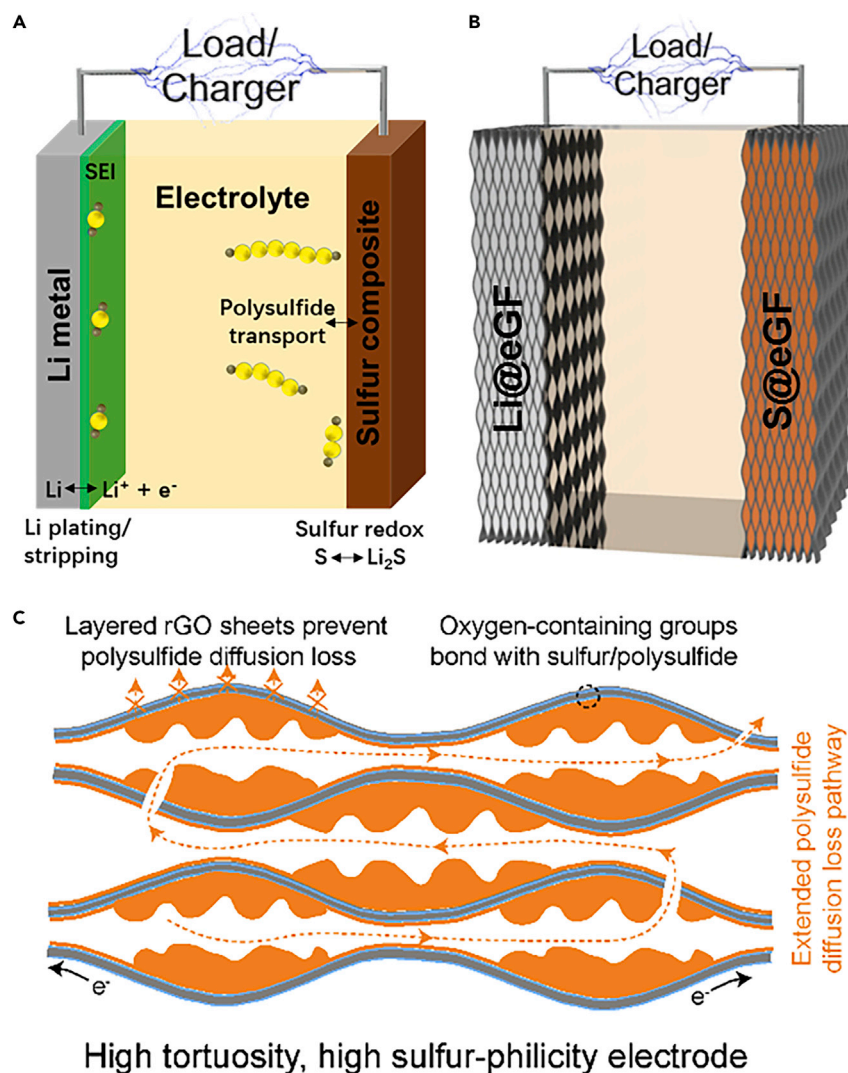


**Figure 1. Schematic of Battery Configurations and Electrode Design**

(A) Schematic of a traditional Li-S battery comprised of a Li metal anode and a sulfur composite cathode.

(B) Schematic of a new-type Li-S battery based on a horizontally aligned, high-tortuosity, and high-affinity rGO host.

(C) Schematic of the electrode design functionality in S@eGF.

electrochemical performance:<sup>2,3</sup> (1) during redox reaction process, the active S and Li<sub>2</sub>S discharge products are electron- and ion-insulated, along with huge structure variation; (2) the serious shuttle effect of dissolved polysulfide intermediates leads to sulfur loss, low Coulombic efficiency, and side reaction with Li; and (3) the unstable solid-electrolyte interface (SEI) on anode surface causes serious Li loss and dendrite formation especially at high rates. To solve these issues, re-

searchers have developed various efficient strategies to improve electrochemical performances, including the design of sulfur host materials for higher sulfur utilization and preventing shuttling of polysulfides (e.g., functional carbon, metal-organic frameworks, and nanostructured inorganic metal oxides/sulfides), the modification of separators (the modified materials are similar with the above-mentioned host materials), the design of new electrolytes with additives to form

stable SEI or low polysulfide solubility, and the protection of Li anode (e.g., artificial SEI).<sup>4</sup> For example, Li et al. reported a nitrogen-doped graphene/TiN nanowire composite as a strong polysulfide anchor for Li-S batteries.<sup>5</sup> Bai et al. developed a HKUST-1-coated graphene-oxide separator to selectively tunnel Li<sup>+</sup> ions but not polysulfide anions.<sup>6</sup> However, these inactive anchor materials lower the cell-level energy density.

In the past decade, although great progress in Li-S battery has been made in terms of the electrodes and electrolytes, great challenges still exist in achieving practical applications.<sup>7</sup> To follow the principles of commercial Li-ion batteries and realize practical Li-S battery, the electrochemical performances should be evaluated and analyzed under realistic conditions as follows: high cathode loading, low negative to positive electrode capacity ratio, and low electrolyte weight to capacity ratio.<sup>8</sup> Considering these important parameters in Li-S battery is of great significance for both fundamental studies and practical applications.

In this issue of *Matter*, Chen et al. report a freestanding one-for-all electrode design by simultaneously engineering the tortuosity and sulfur-affinity of a reduced graphene-oxide (rGO) host for high-performance Li-S batteries (Figure 1B).<sup>9</sup> For the S cathode, this smart architecture not only mitigates the diffusion/dissolution sulfur loss due to the strong bonding from rich oxygen functional groups, but also confines the soluble polysulfide through prolonged diffusion pathways caused by high tortuosity (Figure 1C). For the Li metal anode, this architecture coupling with molten Li can efficiently suppress the formation of Li dendrites. Additionally, the resulting electrodes without binders and carbon additives exhibit fast electronic/ionic diffusion. It is noteworthy that the high-tortuosity and high-affinity architecture was successfully synthesized by milliseconds

treating of a freestanding and densely stacked graphene-oxide film at high temperature, demonstrating its facile and efficient synthesis strategy. The heat-triggered ultrafast self-expansion and reduction reaction generates gases and internal pressure between rGO layers, thus resulting in the formation of high-tortuosity rGO with nanogaps. Due to the high sulfur philicity and strong capillary force in nanogaps, sulfur, and lithium can rapidly and uniformly infiltrate into the architecture.

To confirm the influences of high tortuosity and high sulfur philicity on Li-S battery performance, another two low-tortuosity and/or low-sulfur-philicity electrodes were designed for comparison. As a proof-of-concept application, the high-tortuosity and high-sulfur-philicity cathode (S@eGF) exhibits higher specific capacity, lower overpotential, superior rate performance, and better cycling stability than other two electrodes. Additionally, through visualizing using a transparent H-cell, the high-tortuosity and high-sulfur-philicity cathode displayed negligible color change in the electrolyte due to very limited polysulfide dissolution/diffusion, indicating the importance of the electrode architecture. Furthermore, to add benefits on its practical applications for Li-S batteries, the cathode was evaluated under high active material loading and at lean electrolyte. At low electrolyte amount of 5~7  $\mu\text{L}$   $\text{mg}_{\text{sulfur}}^{-1}$ , this cathode can achieve high areal capacities of 13.7, 15, and 21  $\text{mAh cm}^{-2}$  at high sulfur loadings of 12, 15, and 20  $\text{mg cm}^{-2}$ , respectively, with high Coulombic efficiency of over 98%. After cycling, uniformly distributed sulfur species and well-

maintained sandwich-like morphology across the electrode demonstrate its successful suppression of polysulfides dissolution/diffusion and sulfur loss.

It is well known that the lithium-dendrite-induced short-circuit problem is also a major bottleneck toward safe, long-life Li-S batteries, especially at ultrahigh sulfur loadings. By using the same rGO host, the resulting molten Li-containing composite anode (Li@eGF) can efficiently accommodate the "infinite" volume change and decrease the areal current density. Combining the merits on both cathode and anode, the assembled full cell achieved a high energy density of 395  $\text{Wh kg}^{-1}$  at a high cathode mass loading of 22  $\text{mg cm}^{-2}$ , low electrolyte amount of 3.5  $\mu\text{L mg}_{\text{sulfur}}^{-1}$ , and less Li amount of 13  $\text{mg cm}^{-2}$ . It was concluded that a high-tortuosity and high-philicity principle in one-for-all electrodes plays a crucial role and provides a guideline for future efforts in rationally designing electrodes for high-performance Li-S batteries.

This work not only solves the major problems of polysulfide diffusion/loss and Li dendrites in Li-S batteries but also presents a state-of-the-art prototype for practical Li-S batteries. Nevertheless, in spite of the breakthrough reported herein on Li-S battery electrodes, future effort is required to achieve high-performance Li-S batteries with lower cost and higher energy density and to replace commercial Li-ion batteries.<sup>10</sup> The cost of Li-S battery mainly comes from raw materials, electrode fabrication processes, battery assembly process, and electrolytes, all of which deserve considerations. On the other hand, next-generation Li-S battery is promising to reach higher energy den-

sity over 500  $\text{Wh kg}^{-1}$  at pouch cell level and meet increasing energy demands. Therefore, although the path toward practical Li-S batteries is tortuous, the vision is not.

1. Fan, L., Li, M., Li, X., Xiao, W., Chen, Z., and Lu, J. (2019). Interlayer Material Selection for Lithium-Sulfur Batteries. *Joule* 3, 361–386.
2. Pang, Q., Liang, X., Kwok, C.Y., and Nazar, L.F. (2016). Advances in Lithium-Sulfur Batteries based on Multifunctional Cathodes and Electrolytes. *Nat. Energy* 1, 16132.
3. Manthiram, A., Chung, S.-H., and Zu, C. (2015). Lithium-sulfur batteries: progress and prospects. *Adv. Mater.* 27, 1980–2006.
4. Pang, Q., Shyamsunder, A., Narayanan, B., Kwok, C.Y., Curtiss, L.A., and Nazar, L.F. (2018). Tuning the Electrolyte Network Structure to Invoke Quasi-Solid State Sulfur Conversion and Suppress Lithium Dendrite Formation in Li-S Batteries. *Nat. Energy* 3, 783–791.
5. Li, Z., He, Q., Xu, X., Zhao, Y., Liu, X., Zhou, C., Ai, D., Xia, L., and Mai, L. (2018). A 3D Nitrogen-Doped Graphene/TiN Nanowires Composite as a Strong Polysulfide Anchor for Lithium-Sulfur Batteries with Enhanced Rate Performance and High Areal Capacity. *Adv. Mater.* 30, e1804089.
6. Bai, S., Liu, X., Zhu, K., Wu, S., and Zhou, H. (2016). Metal-Organic Framework-based Separator for Lithium-Sulfur Batteries. *Nat. Energy* 1, 16094.
7. Chen, X., Hou, T., Persson, K.A., and Zhang, Q. (2019). Combining Theory and Experiment in Lithium-Sulfur Batteries: Current Progress and Future Perspectives. *Mater. Today* 22, 142–158.
8. Niu, C., Pan, H., Xu, W., Xiao, J., Zhang, J.-G., Luo, L., et al. (2019). Self-Smoothing Anode for Achieving High-Energy Lithium Metal Batteries under Realistic Conditions. *Nat. Nanotechnol.* 14, 594–601.
9. Chen, H., Zhou, G., Boyle, D., Wan, J., Wang, H., Lin, D., Mackanic, D., Zhang, Z., Kim, S.C., Lee, H.R., et al. (2020). Electrode Design with Integration of High Tortuosity and Sulfur-Philicity for High Performance Lithium-Sulfur Battery. *Matter* 2, this issue, 1605–1620.
10. Chung, S.-H., and Manthiram, A. (2018). Designing Lithium-Sulfur Cells with Practically Necessary Parameters. *Joule* 2, 710–724.